Inorg. Chem. **2005**, *44*, 559–565

Controlled Aggregation of Heterometallic Nanoscale $Cu_{12}Ln_6$ Clusters (Ln = Gd^{III} or Nd^{III}) into 2D Coordination Polymers

Feng He, Ming-Liang Tong, Xiao-Lan Yu, and Xiao-Ming Chen*

School of Chemistry and Chemical Engineering, Sun Yat-Sen University, Guangzhou 510275, P. R. China

Received September 6, 2004

Discrete dinuclear and polymeric heterometallic copper(II)–lanthanide(III) complexes have been synthesized upon variation of pH and characterized by X-ray diffraction analysis. Reactions of the ligand Htza (tetrazole-1-acetic acid) with copper(II) and lanthanide(III) salts gave dinuclear $[CuLn(tza)_4(H_2O)_5Cl]$ complexes at the low pH of 3.5 and 2D heterometallic coordination polymers with high-nuclearity $[\{Cu_2(OH)_2\}_2\{Cu_{12}Ln_6(\mu_3\text{-}OH)_{24}(Cl)_{1/2}(NO_3)_{1/2}\text{-}(tza)_{12}(H_2O)_{18}\}](NO_3)_9\cdot 8H_2O$ (Ln = Gd or Nd) at a higher pH of 6.6. The acidity of the reaction solution can cause drastic changes in the structures of the products. In the dinuclear complexes, each pair of adjacent dinuclear molecules is linked through hydrogen bonds and π–π stacking interactions, and the whole structure is a hydrogen-bonded three-dimensional cubic net. In the coordination polymers, the connecting nodes are $[Cu_{12}Ln_6]$ units, which are interconnected by $[Cu_2O_2]$ units into two-dimensional structures. Magnetic studies exhibit the existence of weak exchange interactions between the Cu^{II} and Ln^{III} ions bridged by carboxylate and hydroxy ligands.

Introduction

There has been growing interest in recent years in the design and synthesis of high-nuclearity complexes motivated by their fascinating structures[1] and rich physical properties.[2−4] In contrast, rational synthesis of multidimensional polymers involving heterometallic high-nuclearity clusters linked by organic ligands is still a challenge in chemistry,[5] and the synthetic difficulties restrict further studies of their chemical and physical properties.[6] In fact, homometallic 4f cluster-based coordination polymers[7] and heterometallic 3d−4f cluster-based,[8,9] especially high-nuclearity-based, coordination polymers are seldomly reported.[10] In the field of heterometallic 3d−4f coordination chemistry,[11,12] we reported

* Author to whom correspondence should be addressed. E-mail: cescxm@zsu.edu.cn. Fax: Int. code +86 20 8411-2245.

(1) (a) Müller, A. *Science* **2003**, *300*, 749−750. (b) Dearden, A. L.; Parsons, S.; Winpenny, R. E. P. *Angew. Chem., Int. Ed.* **2001**, *40*, 151−154. (c) Fenske, D.; Persau, C.; Dehnen, S.; Anson, C. E. *Angew. Chem., Int. Ed.* **2004**, *43*, 305−309.

(2) (a) Ford, P. C.; Cariati, E.; Bourassa, J. *Chem. Rev.* **1999**, *99*, 3625−3648. (b) Yam, V. W.-W.; Lo, K. K.-W. *Chem. Soc. Rev.* **1999**, *28*, 323−334.

(3) (a) Brockman, J. T.; Huffman, J. C.; Christou, G. *Angew. Chem., Int. Ed.* **2002**, *41*, 2506−2508. (b) Brechin, E. K.; Boskovic, C.; Wernsdorfer, W.; Yoo, J.; Yamaguchi, A.; Sanudo, E. C.; Concolino, T. R.; Rheingold, A. L.; Ishimoto, H.; Hendrickson, D. N.; Christou, G. *J. Am. Chem. Soc.* **2002**, *124*, 9710−9711.

(4) Müller, A.; Serain, C. *Acc. Chem. Res.* **2000**, *33*, 2−10.

(5) (a) Eddaoudi, M.; Kim, J.; Rosi, N.; Vodak, D.; Wachter, J.; O'Keeffe, M.; Yaghi, O. M. *Science* **2002**, *295*, 469−472. (b) Miyasaka, H.; Nakata, K.; Sugiura, K.; Yamashita, M.; Clérac, R. *Angew. Chem., Int. Ed.* **2004**, *43*, 707−711. (c) Zheng, N.-F.; Bu, X.-H.; Feng, P.-Y. *J. Am. Chem. Soc.* **2002**, *124*, 9688−9689.

(6) (a) Eddaoudi, M.; Moler, D. B.; Li, H.; Chen, B.; Reineke, T. M.; O'Keeffe, M.; Yaghi, O. M. *Acc. Chem. Res.* **2001**, *34*, 319−330. (b) Selby, H. D.; Roland, B. K.; Zheng, Z.-P. *Acc. Chem. Res.* **2003**, *36*, 933−944.

(7) (a) Ma, B.-Q.; Zhang, D.-S.; Gao, S.; Jin, T.-Z.; Yan, C.-H.; Xu, G.-X. *Angew. Chem., Int. Ed.* **2000**, *39*, 3644−3646. (b) Wang, R. Y.; Liu, H.; Carducci, M. D.; Jin, T. Z.; Zheng, C.; Zheng, Z. P. *Inorg. Chem.* **2001**, *40*, 2743−2750. (c) Zheng, Z. P. *Chem. Commun.* **2001**, 2521−2529. (d) Zhou, Y.-F.; Jiang, F.-L.; Yuan, D.-Q.; Wu, B.-L.; Wang, R.-H.; Lin, Z.-Z.; Hong, M.-C. *Angew. Chem., Int. Ed.* **2004**, *43*, 5665−5668.

(8) (a) Kou, H.-Z.; Zhou, B.-C.; Wang, R.-J. *Inorg. Chem.* **2003**, *42*, 7658−7665. (b) Ren, Y.-P.; Long, L.-S.; Mao, B.-W.; Yuan, Y.-Z.; Huang, R.-B.; Zheng, L.-S. *Angew. Chem., Int. Ed.* **2003**, *42*, 532−535. (c) Liu, S. M.; Meyers, E. A.; Shore, S. G. *Angew. Chem., Int. Ed.* **2002**, *41*, 3609−3611. (d) Novitchi, G.; Shova, S.; Caneschi, A.; Costes, J.-P.; Gdaniec, M.; Stanica, N. *J. Chem. Soc., Dalton Trans.* **2004**, 1194−1200.

(9) (a) Rizzi, A. C.; Calvo, R.; Baggio, R.; Garland, M. T.; Pena, O.; Perec, M. *Inorg. Chem.* **2002**, *41*, 5609−5614. (b) Liang, Y. C.; Cao, R.; Su, W. P.; Hong, M. C.; Zhang, W. J. *Angew. Chem., Int. Ed.* **2000**, *39*, 3304−3307. (c) Mao, J. G.; Song, L.; Huang, X. Y.; Huang, J. S. *Polyhedron* **1997**, *16*, 963−966.

(10) (a) Zhang, J. J.; Xia, S. Q.; Sheng, T. L.; Hu, S. M.; Leibeling, G.; Meyer, F.; Wu, X. T.; Xiang, S. C.; Fu, R. B. *Chem. Commun.* **2004**, 1186−1187. (b) Zhang, J. J.; Sheng, T. L.; Hu, S. M.; Xia, S. Q.; Leibeling, G.; Meyer, F.; Fu, Z. Y.; Chen, L.; Fu, R. B.; Wu, X. T. *Chem.—Eur. J.* **2004**, *43*, 3963−3969. (c) Zhang, J. J.; Sheng, T. L.; Xia, S. Q.; Leibeling, G.; Meyer, F.; Hu, S.-M.; Fu, R.-B.; Xiang, S. C.; Wu, X.-T. *Inorg. Chem.* **2004**, *43*, 5472−5478. (d) Hu, S.-M.; Dai, J.-C.; Wu, X.-T.; Wu, L.-M.; Cui, C.-P.; Fu, Z.-Y.; Hong, M.-C.; Liang, Y.-C. *J. Cluster Sci.* **2002**, *13*, 33−41.

10.1021/ic048754s CCC: $30.25
Published on Web 01/13/2005

Scheme 1. Assembly Strategy

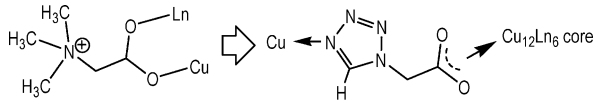

the synthesis and magnetic investigations of a series of discrete heterometallic $Cu^{II}-Ln^{III}$ (Ln = lanthanide) complexes using betaine (i.e. trimethylammonioacetate) and its derivatives in the past decade,[13−15] demonstrating a crucial role of the reaction pH in the formation of these clusters.[16] As an expansion of the synthetic strategy to develop 3d−4f complexes chemistry, we attempted to construct multidimensional arrays and networks containing highly aggregate clusters as nodes and hope to provide useful information for the novel structures. Among them, the unusual nanosized $[Cu_{12}Ln_6]$ cores[14] bridged by μ_3-OH^- and carboxylate groups attracted our interest in assembly of them into nanoscale cluster-based frameworks. Obviously, if the hanging monocarboxylate ligand could be replaced by an appropriate exobidentate ligand, a new synthetic approach may be established for interlinking of such nanosized clusters into higher dimensional networks with intriguing structural features and useful physical properties.

We selected a multifunctional ligand, tetrazole-1-acetic acid (designated as Htza) with both carboxylate and tetrazole ends, to replace betaines (Scheme 1). The employment of this ligand was found to generate dinuclear $[CuLn(tza)_4(H_2O)_5Cl]$ (Ln = Gd or Nd) complexes at a low pH of 3.5. According to our previous acidity control approach,[16] we were then able to isolate unusual two-dimensional (2D) networks based on the nanosized clusters $[\{Cu_2(OH)_2\}_2\{Cu_{12}Ln_6(\mu_3\text{-}OH)_{24}(Cl)_{1/2}(NO_3)_{1/2}(tza)_{12}(H_2O)_{18}\}](NO_3)_9\cdot 8H_2O$ (Ln = Gd (**2**·Gd) or Nd (**2**·Nd)) by mixing $CuCl_2$ and $Ln(NO_3)_3$ (Ln = Gd or Nd) at a higher pH of 6.6. We now report herein the synthesis, crystal structures, and magnetic properties of the neutral dinuclear complexes and the 2D networks based on the nanosized clusters.

Experimental Section

Chemicals were used as purchased from commercial vendors without further purification. The C, H, and N microanalyses were carried out with a Perkin-Elmer 240Q elemental analyzer. FT-IR spectra were recorded from KBr pellets in the range of 4000−400 cm^{-1} on a Nicolet 5DX spectrometer. The variable-temperature magnetic-susceptibility data were measured with a Quantum Design MPMS7 SQUID magnetometer. Diamagnetic corrections were made with Pascal's constants.[17]

Preparation. $CuGd(tza)_4(H_2O)_5Cl$ (1·Gd). A mixture of Htza (0.256 g, 2.0 mmol) and $CuCl_2\cdot 2H_2O$ (0.170 g, 1.0 mmol) was dissolved in distilled water (5 mL), and the solution was heated at 60 °C for 10 min; $Gd(NO_3)_3\cdot 5H_2O$ (0.433 g, 1.0 mmol) was then added. The pH was adjusted to 3.5 with KOH solution, and the resulting blue solution was allowed to stand in air at room temperature for about 1 week, yielding beautiful blue polyhedral crystals (yield 82%). Anal. Calcd for **1**·Gd: C, 16.86; H, 2.59; N, 26.22. Found: C, 16.79; H, 2.61; N, 26.18. IR data (ν/cm^{-1}): 3359.9 s br, 3169.8 s, 3015.1 m, 2938.9 w, 1694.8 s, 1615.3 s, 1453.8 w, 1405.7 s, 1328.1 m, 1272.6 w, 1186.3 m, 1148.9 m, 1115.1 m, 1049.2 w, 986.7 m, 812.9 m, 704.7 s, 653.1 m, 579.2 m, 505.2 w.

$CuNd(tza)_4(H_2O)_5Cl$ (1·Nd). This was prepared as for **1**·Gd (yield 81%). Anal. Calcd for **1**·Nd: C, 17.13; H, 2.63; N, 26.63. Found: C, 17.07; H, 2.75; N, 26.48. IR data (ν/cm^{-1}): 3359.7 s br, 3170.1 s, 3015.6 w, 2937.8 w, 1695.3 s, 1614.2 m, 1453.7 m, 1405.8 s, 1327.1 m, 1272.5 m, 1186.0 m, 1148.7 w, 1114.9 m, 1047.3 w, 986.6 m, 812.2 m, 703.5 s, 652.2 m, 579.1 m, 504.8 w.

$[\{Cu_2(OH)_2\}_2\{Cu_{12}Gd_6(\mu_3\text{-}OH)_{24}(Cl)_{1/2}(NO_3)_{1/2}(tza)_{12}(H_2O)_{18}\}](NO_3)_9\cdot 8H_2O$ (2·Gd). $CuCl_2\cdot 2H_2O$ (0.170 g, 1.0 mmol), $Gd(NO_3)_3\cdot 5H_2O$ (0.433 g, 1.0 mmol), and Htza (0.256 g, 2.0 mmol) were mixed in distilled water (15.6 mL), and the mixture was stirred at about 86 °C for 1 h. An aqueous KOH solution (1 M) was then added dropwise to cause a slight precipitate. The mixture was stirred for 24 h and then filtered. The filtrate (pH = 6.6) was allowed to slowly concentrate by evaporation at ambient temperature over 40 days, and the resulting blue polyhedral crystals (yield 16%) were collected by filtration. Anal. Calcd for **1**·Gd: N, 15.99; C, 8.59; H, 2.32. Found: N, 16.15; C, 8.82; H, 2.38. IR data (ν/cm^{-1}): 3359.5 s, 3169.2 s, 2938.6 m, 1694.2 s, 1405.3 s, 1327.7 m, 1185.9 m, 1114.4 m, 704.1 s.

$[\{Cu_2(OH)_2\}_2\{Cu_{12}Nd_6(\mu_3\text{-}OH)_{24}(Cl)_{1/2}(NO_3)_{1/2}(tza)_{12}(H_2O)_{18}\}](NO_3)_9\cdot 8H_2O$ (2·Nd). The synthetic method was similar to that for **2**·Gd by using $Nd(NO_3)_3$ instead of $Gd(NO_3)_3$. Yield: 18%. Anal. Calcd for **2**·Nd: N, 16.24; C, 8.72; H, 2.36. Found: N, 16.21; C, 8.45; H, 2.41. IR data (ν/cm^{-1}): 3359.8 s, 3169.6 s, 2938.2 m, 1694.8 s, 1405.5 s, 1327.9 m, 1186.1 m, 1114.8 m, 704.8 s.

X-ray Crystallography. A summary of selected crystallographic data for **1**·Gd, **1**·Nd, **2**·Gd, and **2**·Nd is given in Table 1. The data collections were carried out on a Bruker SMART Apex CCD diffractometer using graphite-monochromated Mo Kα radiation (λ = 0.710 73 Å) at 293 K by using frames of 0.3° oscillation ($4.3 \le 2\theta \le 60°$). Absorption corrections were applied by using SADABS.[18] The structures were solved with direct methods and refined by full-matrix least-squares techniques with the SHELXTL programs.[19] The anions encapsulated at the cage of the octadecanuclear $Cu_{12}Ln_6$ cluster in **2**·Gd or **2**·Nd were refined to be half a Cl^- and half a disordered NO_3^- anion. Anisotropic thermal parameters were applied to all non-hydrogen atoms. The organic hydrogen atoms were generated geometrically (C−H 0.96 Å); the aqua hydrogen atoms were located from difference maps and refined with isotropic temperature factors. Selected bond lengths and bond angles are listed in Tables 2 and 3.

(11) (a) Winpenny, R. E. P. *Chem. Soc. Rev.* **1998**, *27*, 447−452. (b) Benelli, C.; Gatteschi, D. *Chem. Rev.* **2002**, *102*, 2369−2387.
(12) (a) Costes, J.-P.; Dahan, F.; Javier, G.-T. *Chem.—Eur. J.* **2002**, *8*, 5430−5434. (b) Osa, S.; Kido, T.; Matsumoto, N.; Re, N.; Pochaba, A.; Mrozinski, J. *J. Am. Chem. Soc.* **2004**, *126*, 420−421.
(13) (a) Chen, X.-M.; Tong, M.-L.; Wu, Y.-L.; Luo, Y.-J. *J. Chem. Soc., Dalton Trans.* **1996**, 2181−2182. (b) Chen, X.-M.; Wu, Y.-L.; Yang, Y.-Y.; Aubin, S. M. J.; Hendrickson, D. N. *Inorg. Chem.* **1998**, *37*, 6186−6191.
(14) Chen, X.-M.; Aubin, S. M. J.; Wu, Y.-L.; Yang, Y.-S.; Mak, T. C. W.; Hendrickson, D. N. *J. Am. Chem. Soc.* **1995**, *117*, 9600−9601.
(15) Yang, Y.-Y.; Huang, Z.-Q.; He, F.; Chen, X.-M.; Ng, S. W. *Z. Anorg. Allg. Chem.* **2004**, *630*, 286−290.
(16) For review, see: Chen, X.-M.; Yang, Y.-Y. *Chin. J. Chem.* **2000**, *18*, 664−672.
(17) Carlin, R. L. *Magnetochemistry*; Springer-Verlag: Berlin, New York, 1986.
(18) Sheldrick, G. M. *Program for Empirical Absorption Correction of Area Detector Data*; University of Göttingen: Göttingen, Germany, 1996.
(19) Sheldrick, G. M. *SHELXTL*, version 6.10; Bruker Analytical X-ray Systems: Madison, WI, 2001.

Table 1. Crystallographic Data and Structure Refinement Parameters for **1**·Gd, **1**·Nd, **2**·Gd, and **2**·Nd

	1·Gd	**1**·Nd	**2**·Gd	**2**·Nd
chem formula	$C_{12}H_{22}ClCuGdN_{16}O_{13}$	$C_{12}H_{22}ClCuGdN_{16}O_{13}$	$C_{36}H_{116}Cl_{0.50}Cu_{16}Gd_6N_{57.50}O_{106.50}$	$C_{36}H_{116}Cl_{0.50}Cu_{16}Nd_6N_{57.50}O_{106.50}$
fw	854.66	841.65	5036.73	4958.67
cryst system	tetragonal	tetragonal	tetragonal	tetragonal
space group	*P4/ncc*	*P4/ncc*	*I4/m*	*I4/m*
a (Å)	10.6062(4)	10.6525(4)	20.3962(4)	20.4620(6)
b (Å)	10.6062(4)	10.6525(4)	20.3962(4)	20.4620(6)
c (Å)	23.9726(13)	24.0415(10)	18.8438(9)	18.9592(10)
V (Å^3)	2696.7(2)	2728.13(18)	7839.1(4)	7938.1(5)
Z	4	4	2	2
ρ_{calcd} (g cm^{-3})	2.105	2.047	2.134	2.075
T (K)	295(2)	295(2)	295(2)	295(2)
λ(Mo Kα) (Å)	0.710 73	0.710 73	0.710 73	0.710 73
μ(Mo Kα) (mm^{-1})	3.418	2.851	4.748	4.144
R_1 ($I > 2\sigma(I)$)[a]	0.0181	0.0200	0.0408	0.0893
wR_2[a]	0.0433	0.0543	0.1328	0.2067

[a] $R_1 = \sum||F_o| - |F_c||/\sum|F_o|$, $wR_2 = [\sum w(|F_o| - |F_c|)^2/\sum w|F_o|^2]^{1/2}$.

Table 2. Selected Bond Lengths (Å) and Angles (deg) for **1**·Gd and **1**·Nd[a]

	1·Gd	**1**·Nd		**1**·Gd	**1**·Nd
Ln(1)−O(3)	2.4207(14)	2.4785(14)	Cu(1)−O(1)	1.9664(14)	1.9694(14)
Ln(1)−O(2)	2.4455(14)	2.4886(14)	Cu(1)−Cl(1)	2.4944(11)	2.4953(11)
Ln(1)−O(4)	2.615(3)	2.621(3)			
O(3)−Ln(1)−O(3)$^{\#1}$	80.44(2)	80.76(2)	O(2)$^{\#1}$−Ln(1)−O(2)	72.15(3)	71.83(3)
O(3)−Ln(1)−O(3)$^{\#3}$	131.89(7)	132.75(6)	O(2)$^{\#2}$−Ln(1)−O(2)$^{\#1}$	112.77(7)	112.11(7)
O(3)−Ln(1)−O(2)$^{\#2}$	140.90(6)	140.36(6)	O(3)−Ln(1)−O(2)	72.59(5)	72.26(5)
O(3)−Ln(1)−O(2)$^{\#1}$	71.05(5)	71.19(5)	O(3)−Ln(1)−O(4)	65.95(3)	66.37(3)
O(3)$^{\#1}$−Ln(1)−O(2)$^{\#1}$	72.59(5)	72.26(5)	O(2)−Ln(1)−O(4)	123.61(3)	123.95(3)
O(3)−Ln(1)−O(2)#3	138.63(5)	138.79(5)	O(1)$^{\#1}$−Cu(1)−O(1)$^{\#2}$	168.73(8)	169.15(8)
O(3)$^{\#1}$−Ln(1)−O(2)	140.90(6)	140.36(6)	O(1)$^{\#1}$−Cu(1)−O(1)	89.448(8)	89.487(8)
O(3)$^{\#2}$−Ln(1)−O(2)	71.05(5)	71.19(5)	O(1)−Cu(1)−Cl(1)	95.63(4)	95.43(4)
O(3)$^{\#3}$−Ln(1)−O(2)	138.63(5)	138.79(5)			

[a] Symmetry codes: (#1) $y, -x + 1/2, z$; (#2) $-y + 1/2, x, z$; (#3) $-x + 1/2, -y + 1/2, z$.

Results and Discussion

Description of Crystal Structures. The crystal structure of **1**·Gd consists of a discrete neutral, dinuclear [CuGd(tza)$_4$(H$_2$O)$_5$Cl] molecule. An ORTEP view of the dinuclear molecule is shown in Figure 1. Both the Cu^{II} and Gd^{III} atoms are located on a crystallographic 4-fold axis. The Cu^{II} ion is coordinated by four carboxylate oxygen atoms at the basal plane [Cu(1)−O 1.967 Å] (Table 1) and completed by a Cl$^-$ ion at the apical position [Cu(1)−Cl(1) 2.494 Å] to exhibit a square-pyramidal geometry. The Gd^{III} ion is quadruply bridged to the Cu^{II} ion by four carboxylate bridges of tza ligands in syn−syn bridging modes [Gd(1)−O 2.4455(14) Å], giving rise to a "paddle-wheel" heterometallic dimer with the Cu···Gd distance of 3.777 Å. This neutral dinuclear structure is somewhat different from the well-known, symmetric "paddle-wheel" structures of copper(II) carboxylates[20] as well as the rare examples of related dinuclear Cu−Ln complexes[21] documented in the literature. Besides the four μ-carboxylate oxygen atoms, the Gd^{III} ion is further coordinated by five aqua ligands [Gd(1)−O = 2.4207(14)−2.615(3) Å] to form nine-coordination, leading to a distorted monocapped square-antiprism, in which one square face consists of four aqua oxygen atoms [O(3), O(3A), O(3B), and O(3C)] whereas the other is defined by four carboxylate oxygen atoms [O(12), O(22), O(32), and O(42)] from the quadruple μ-carboxylate bridges. The dihedral angle between the square faces is ca. 58°.

Hydrogen bonding (Table 4) plays an important role in consolidating the crystal structure of **1**·Gd. As shown in Figure 2, all of the aqua ligands participate in hydrogen bonding with tza nitrogen atoms. Each pair of adjacent dinuclear molecules is linked through two hydrogen bonds between the aqua ligands and the nitrogen atoms of tza ligands [O(3a)···N(3a) 2.794(5) Å], resulting in a 2D (4,4) grid around the *ab* plane with an intermolecular Cu···Cu distance of 10.606(1) Å in the solid. Furthermore, one aqua ligand provides an intermolecular hydrogen bond to the choro ligand (O(4w)···Cl(1) 3.091(5) Å). The above hydrogen-bonded 2D (4,4) grids are then interlinked by such O(4w)···Cl(1) hydrogen bonds perpendicular to the grids into the final hydrogen-bonded 3D cubic net, in which the (4,4) grids are arranged in a roughly "face-to-face" fashion (Figure 2).

The crystal structure of **1**·Nd is isomorphous to that of **1**·Gd; hence, only very small metric differences have been observed for them. Because the radius of a Nd^{III} ion is slightly smaller than that of a Gd^{III} ion, all of the metal−ligand bonds in **1**·Nd are slightly shorter than the corresponding bonds in **1**·Gd, as compared in Table 3. However, the bond angles in both **1**·Gd and **1**·Nd are almost the same.

(20) (a) Harcourt, R. D.; Skrezenek, F. L.; Maclagan, R. G. A. R. *J. Am. Chem. Soc.* **1986**, *108*, 5403. (b) Chen, X.-M.; Feng, X.-L.; Tong, Y.-X.; Zhang, X.-H. *Polyhedron* **1996**, *15*, 3585−3588.

(21) Yang, Y.-Y.; Wu, Y.-L.; Long, L.-S.; Chen, X.-M. *J. Chem. Soc., Dalton Trans.* **1999**, 2005−2009.

Table 3. Selected Bond Lengths (Å) and Angles (deg) for **2**·Gd and **2**·Nd[a]

	2·Gd	**2**·Nd		**2**·Gd	**2**·Nd
Ln(1)−O(4)	2.384(6)	2.433(11)	Cu(1)−O(1H)$^{\#2}$	1.964(3)	1.965(6)
Ln(1)−O(1)	2.427(4)	2.471(7)	Cu(1)−O(3H)	1.984(3)	1.994(7)
Ln(1)−O(2H)	2.462(3)	2.514(6)	Cu(1)−O(1H)	1.992(3)	1.999(6)
Ln(1)−O(1W)	2.466(5)	2.511(10)	Cu(1)−O(2)	2.317(4)	2.335(8)
Ln(1)−O(3H)	2.475(3)	2.513(6)	Cu(2)−O(2H)	1.945(3)	1.953(6)
Ln(1)−O(2W)	2.501(5)	2.559(11)	Cu(2)−O(3H)$^{\#3}$	1.949(3)	1.958(6)
Ln(1)···Cu(2)	3.4892(8)	3.527(2)	Cu(2)−O(3)	2.373(6)	2.391(12)
Ln(1)···Cu(2)$^{\#2}$	3.5047(8)	3.549(2)	Cu(2)···Ln(1)$^{\#5}$	3.5047(8)	3.549(2)
Ln(1)···Cu(1)	3.5253(6)	3.5636(12)	Cu(3)−O(4H)	1.942(4)	1.936(7)
Ln(2)−O(3W)	2.438(4)	2.495(8)	Cu(3)−N(4)	1.979(5)	1.985(10)
Ln(2)−O(1H)	2.464(3)	2.508(7)	Cu(3)···Cu(3)$^{\#6}$	2.868(2)	2.873(4)
Ln(2)−O(4W)	2.473(9)	2.488(2)	O(1H)−Cu(1)$^{\#3}$	1.964(3)	1.965(6)
Ln(2)···Cu(1)	3.5346(7)	3.5720(13)	O(3H)−Cu(2)$^{\#2}$	1.949(3)	1.958(6)
Cu(1)−O(2H)	1.944(3)	1.943(7)	O(4H)−Cu(3)#6	1.942(4)	1.936(7)
O(4)−Ln(1)−O(1)$^{\#1}$	84.37(10)	84.8(2)	O(2H)−Cu(1)−O(1H)$^{\#2}$	175.89(15)	175.5(3)
O(1)$^{\#1}$−Ln(1)−O(1)	142.55(17)	144.0(3)	O(2H)−Cu(1)−O(3H)	84.59(14)	85.3(3)
O(4)−Ln(1)−O(2H)	74.47(14)	74.3(3)	O(1H)$^{\#2}$−Cu(1)−O(3H)	95.46(14)	95.0(3)
O(1)$^{\#1}$−Ln(1)−O(2H)	136.57(12)	136.0(2)	O(2H)−Cu(1)−O(1H)	95.24(14)	94.3(3)
O(1)−Ln(1)−O(2H)	73.19(12)	72.8(2)	O(1H)$^{\#2}$−Cu(1)−O(1H)	84.48(19)	85.1(4)
O(2H)−Ln(1)−O(2H)$^{\#1}$	64.8(2)	64.5(3)	O(3H)−Cu(1)−O(1H)	176.89(14)	176.4(3)
O(4)−Ln(1)−O(1W)	138.6(2)	139.8(4)	O(2H)−Cu(1)−O(2)	85.99(15)	86.8(3)
O(1)−Ln(1)−O(1W)	82.62(10)	83.0(2)	O(1H)$^{\#2}$−Cu(1)−O(2)	98.11(16)	97.7(3)
O(2H)−Ln(1)−O(1W)	136.90(11)	136.3(2)	O(3H)−Cu(1)−O(2)	91.73(15)	91.7(3)
O(4)−Ln(1)−O(3H)	137.09(11)	136.6(2)	O(1H)−Cu(1)−O(2)	91.36(15)	91.8(3)
O(1)#1−Ln(1)−O(3H)	135.14(12)	134.5(2)	O(2H)$^{\#1}$−Cu(2)−O(2H)	85.5(2)	86.7(4)
O(1)−Ln(1)−O(3H)	71.94(12)	71.8(2)	O(2H)−Cu(2)−O(3H)$^{\#5}$	174.89(15)	174.9(3)
O(2H)−Ln(1)−O(3H)	64.76(11)	64.1(2)	O(2H)−Cu(2)−O(3H)$^{\#3}$	93.96(15)	93.3(3)
O(2H)$^{\#1}$−Ln(1)−O(3H)	98.64(11)	97.6(2)	O(3H)$^{\#5}$−Cu(2)−O(3H)$^{\#3}$	86.1(2)	86.3(4)
O(1W)−Ln(1)−O(3H)	74.13(13)	74.0(2)	O(2H)−Cu(2)−O(3)	89.30(14)	89.8(3)
O(3H)−Ln(1)−O(3H)$^{\#1}$	65.08(16)	64.4(3)	O(3H)$^{\#5}$−Cu(2)−O(3)	95.77(14)	95.3(3)
O(4)−Ln(1)−O(2W)	70.2(2)	70.5(4)	O(4H)$^{\#6}$−Cu(3)−O(4H)	84.8(2)	84.2(5)
O(1)−Ln(1)−O(2W)	71.29(9)	72.0(2)	O(4H)−Cu(3)−N(4)	91.94(19)	92.4(4)
O(2H)−Ln(1)−O(2W)	131.47(12)	131.7(2)	O(4H)−Cu(3)−N(4)$^{\#7}$	170.8(3)	171.0(5)
O(1W)−Ln(1)−O(2W)	68.45(19)	69.3(4)	N(4)−Cu(3)−N(4)$^{\#7}$	92.5(3)	92.2(6)
O(3H)−Ln(1)−O(2W)	129.88(12)	130.7(2)	Cu(1)$^{\#3}$−O(1H)−Cu(1)	116.67(18)	117.5(3)
O(3W)$^{\#2}$−Ln(2)−O(3W)$^{\#3}$	139.5(2)	136.4(3)	Cu(1)$^{\#3}$−O(1H)−Ln(2)	105.34(14)	105.3(3)
O(3W)$^{\#2}$−Ln(2)−O(3W)	83.11(7)	83.27(14)	Cu(1)−O(1H)−Ln(2)	104.47(13)	104.3(3)
O(3W)$^{\#2}$−Ln(2)−O(1H)	73.31(14)	73.7(3)	Cu(1)−O(2H)−Cu(2)	122.34(17)	122.9(3)
O(3W)$^{\#3}$−Ln(2)−O(1H)	137.31(14)	136.8(3)	Cu(1)−O(2H)−Ln(1)	105.68(14)	105.4(3)
O(3W)−Ln(2)−O(1H)	73.91(14)	74.0(3)	Cu(2)−O(2H)−Ln(1)	104.09(15)	103.6(3)
O(3W)$^{\#4}$−Ln(2)−O(1H)	136.47(14)	136.4(3)	Cu(2)$^{\#2}$−O(3H)−Cu(1)	119.45(17)	119.5(3)
O(1H)−Ln(2)−O(1H)$^{\#2}$	65.30(9)	64.7(2)	Cu(2)$^{\#2}$−O(3H)−Ln(1)	104.15(14)	104.4(3)
O(1H)−Ln(2)−O(1H)$^{\#4}$	99.46(16)	98.3(3)	Cu(1)−O(3H)−Ln(1)	103.95(13)	103.9(3)
O(3W)−Ln(2)−O(4W)	69.74(11)	70.0(2)	Cu(3)$^{\#6}$−O(4H)−Cu(3)	95.2(2)	95.8(5)
O(1H)−Ln(2)−O(4W)	130.27(8)	130.87(15)			

[a] Symmetry codes: (#1) $x, y, -z$; (#2) $-y, x, z$; (#3) $y, -x, z$; (#4) $-x, -y, z$; (#5) $y, -x, -z$; (#6) $-x, -y + 1, -z$; (#7) $-x, -y + 1, z$.

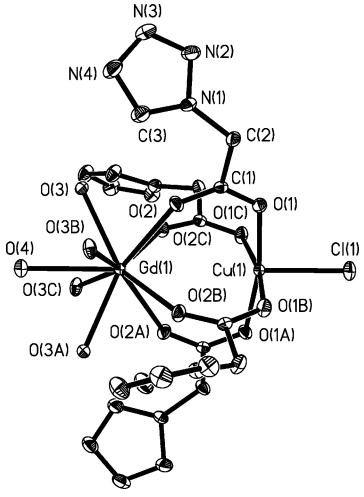

Figure 1. ORTEP drawing (at 30% probability level) of the dinuclear molecule in **1**·Gd.

In **2**·Nd and **2**·Gd there are both heterometallic octadecanuclear $Cu_{12}Ln_6$ subunits and dinuclear $Cu_2(\mu\text{-OH})_2$ subunits. X-ray structural analysis reveals that **2**·Nd and **2**·Gd are isostructural and only minor geometric differences are found. Therefore, only the structure of **2**·Gd is described here. The $Cu_{12}Gd_6$ subunit in a 4/*m* site symmetry, which is the highest symmetry among such kinds of octadecanuclear cores, is slightly different from those found in our previously prepared discrete complexes.[14] In this octadecanuclear core, 6 Gd^{III} ions are positioned at the vertexes of a regular octahedron and the 12 Cu^{II} ions are located at the midpoints of the 12 octahedral edges (Figure 3). This Cu−Gd metal framework is interconnected by 24 similar μ_3-OH ligands

Table 4. Hydrogen Bonds in **1**·Gd (D, Donor Atom; A, Acceptor Atom)[a]

D−H···A	*d*(D−H) (Å)	*d*(H···A) (Å)	D−H···A (deg)	*d*(D···A) (Å)
O3−H3$^{\#1}$···N4	0.85	2.129	142.47	2.85
O3−H3$^{\#2}$···N3	0.85	1.955	169.25	2.79

[a] Symmetry codes: (#1) $y + 1/2, x - 1/2, -z + 1/2$; (#2) $-x + 1/2, -y - 1/2, z$.

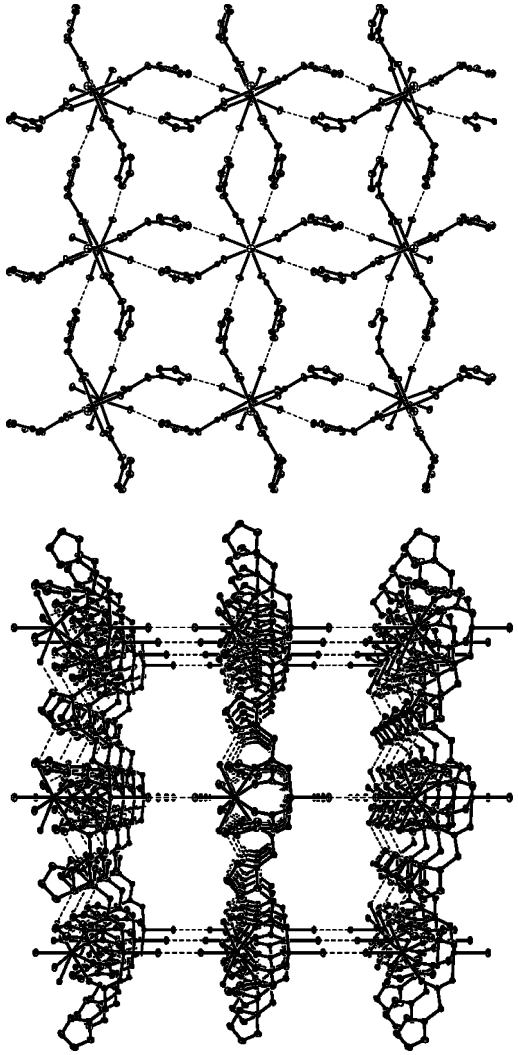

Figure 2. Views of hydrogen-bonded 2D (upper) and 3D (lower) networks of **1**·Gd along the *c*-axis and *a*-axis, respectively.

that are each linked to one Gd^{III} ion (Gd−O 2.462(3)−2.475(3) Å) and two Cu^{II} ions (Cu−O 1.944(3)−1.992(3) Å); each Gd(μ_3-OH)$_4$ fragment is square-pyramidal, and each Cu(μ_3-OH)$_4$ fragment is square-planar. Each Gd^{III} ion is nine-coordinated in a monocapped square-antiprismatic geometry. There are two types of Gd^{III} coordination environments: each of the four Gd^{III} atoms at the equatorial plane of octahedron is coordinated by four O atoms from μ_3-OH and three O atoms from three tza μ-carboxylate-*O*,*O*′ ends and two aqua ligands, whereas each of the two Gd^{III} ions at the apical positions is ligated by four O atoms from μ_3-OH and five aqua ligand. Different from the previously reported discrete $Cu_{12}Ln_6$ clusters,[14] two axial Gd^{III} atoms at the octahedron are not ligated by the carboxylate group. Each Cu^{II} ion is ligated in a square-pyramidal geometry with four μ_3-OH groups in the basal plane and one tza carboxylate oxygen atom at the apical position (Cu−O 2.317(4)−3.379(5) Å). In the $Cu_{12}Ln_6$ core, each pair of the adjacent Cu···Cu is linked by a single OH^- group bridge with the Cu···Cu distances in the range 3.307(2)−3.407(2) Å. Each Gd^{III} ion is linked to four adjacent Cu^{II} atoms by four μ_3-OH bridges with the Cu···Gd separations of 3.489(1)−3.535(1) Å, and

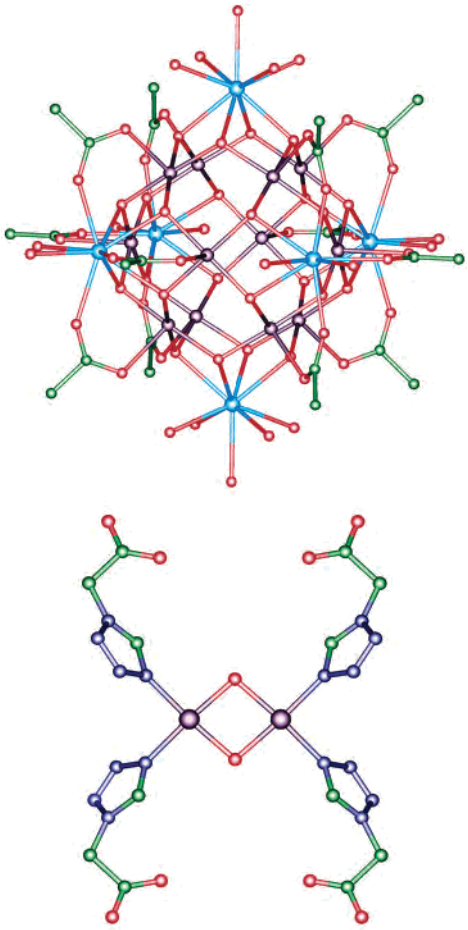

Figure 3. Perspective drawing of a [$Cu_{12}Gd_6$] (tetrazole groups omitted for clarity) (top) and a dinuclear $Cu_2(OH)_2(tza)_4$ subunit (bottom) in **2**·Gd.

each pair of Gd^{III} atoms in each edge of the octahedron is separated at distances of 7.02 Å. In the surrounding of the $Cu_{12}Ln_6$ core, there are 12 tza ligands and 18 aqua ligands participating in coordination to the metal atoms. Every tza ligand bridges a Gd^{III} atom (Gd−O 2.384(6)−2.427(4) Å) and a Cu^{II} atom (Cu−O 2.317(4)−2.373(6) Å) through its μ-carboxylate-*O*,*O*′ group. In the cage of the $Cu_{12}Gd_6$ core, there is half a Cl^- and half a disordered NO_3^- anion.

In the rhombic dinuclear, μ-OH-bridged $Cu_2(\mu\text{-}OH)_2$ subunit (Figure 3) in **2**, the Cu^{II} ion has a 4 + 2 elongated octahedral coordination environment and the equatorial positions are occupied by two μ-OH groups (Cu−O 1.942(4) Å) and two tza nitrogen atoms (Cu−N 1.979(5) Å), while the two axial positions are weakly ligated by two tza nitrogen atoms (Cu−N 2.574(4) Å). Within each dinuclear subunits, the Cu−O−Cu bridging angle is at 95.2(2)° with the intradimer Cu···Cu separation of 2.868(2) Å. Such $Cu_2(\mu\text{-}OH)_2$ subunits are important in interlinkage of the $Cu_{12}Gd_6$ subunits. Each $Cu_{12}Gd_6$ cluster, acting as a four-connected node, is linked to four $Cu_2(OH)_2$ subunits by tza ligands; in turn, each $Cu_2(OH)_2$ subunit is bound to two neighboring $Cu_{12}Gd_6$ units in a linear arrangement. Hence the tza ligand acts as an organic bridge to link two kinds of cluster subunits (Figure 4). By this way, a 2D (4,4) square net with the unit size of 20.396(2) × 20.396(2) Å and cavity size of ca. 13.7 × 13.7 Å is generated with the $Cu_2(OH)_2(tza)_4$ fragment

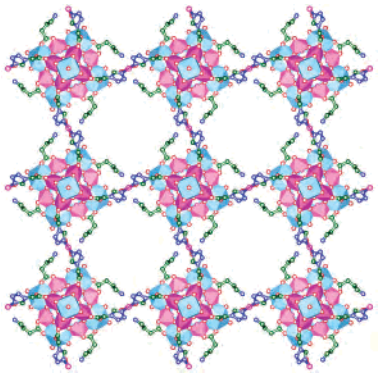

Figure 4. Perspective drawing of the 2D Network in **2**·Gd viewed along the *c*-axis.

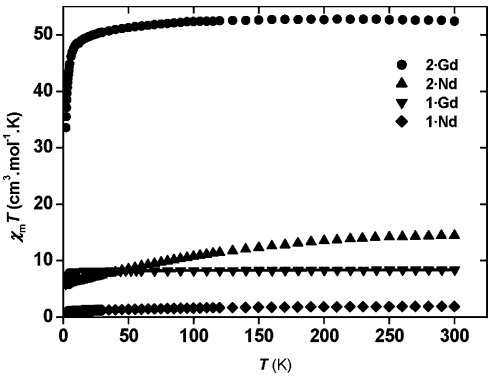

Figure 5. Plots of $\chi_M T$/mol vs temperature for **1**·Gd, **1**·Nd, **2**·Gd, and **2**·Nd. The solid line represents the best theoretical fit for **1**·Gd.

regarded as a metallolinker. Unfortunately, the layers are stacked along the *c*-axis in an ABAB sequence with the lattice water molecules located within and between the layers, excluding the formation of a porous structure in the solid.

Magnetic Properties. The variable-temperature magnetic susceptibility data for the four complexes were measured in the temperature range 2−300 K in an applied magnetic field of 10 kG (Figure 5), while those of **1**·Gd and **2**·Gd in an applied magnetic field of 1.0 kG are basically the same as the corresponding curves measured in an applied magnetic field of 10 kG. For **1**·Gd, the value of $\chi_M T$ is 8.4 cm^3 K mol^{-1} at 300 K and remains practically constant to 11 K. On further lowering of the temperature, $\chi_M T$ decreases more rapidly and equals 5.90 cm^3 K mol^{-1} at 2 K. For **1**·Nd, the value of $\chi_M T$ is 1.9 cm^3 K mol^{-1} at 300 K and decreases continuously to a value of 0.87 cm^3 K mol^{-1}. The $\chi_M T$ values of **1** at high temperature are very close to the values calculated on the basis of the free-ion approximation for Ln^{III} and Cu^{II}, indicating no strong magnetic exchange interaction between adjacent Ln^{III} ions and Cu^{II} ions. For **1**·Gd, the data over the whole temperature range 2−300 K are well fitted to the Curie−Weiss law with $C = 8.39$ and $\Theta = -0.79$ K; such behavior can be referred to the presence of a very weak antiferromagnetic interaction between Cu^{II} and Gd^{III} ions. Taking into consideration the occurrence of intramolecular magnetic interactions (J) and intermolecular interactions (J'), we tried to fit the experimental data for **1**·Gd using the literature expression,[8d] leading to the following set of parameters: $g_{Gd} = 1.99(2)$, $g_{Cu} = 2.03(1)$; $J = -0.37(1)$ cm^{-1}, $J' = -0.012(6)$ cm^{-1}; agreement factor $R = 1.8 \times 10^{-5}$ (Figure 5). This fitting indicates a weak, intramolecular Cu−Gd antiferromagnetic interaction. For **1**·Nd, the data in the range 35−300 K can be fitted to the Curie−Weiss law with $C = 2.08$ and $\Theta = -27.28$ K. Such decrease of $\chi_M T$ should mainly be in fact due to crystal-field effects around the Nd^{III} ion, similar to those reported previously.[22b,25] It is well-known that the depopulation of the Nd Stark levels as temperature decreases is a distinct magnetic phenomenon. The $^4I_{9/2}$ free-ion ground state in the crystal field is split into five Kramers doublets.[23] At room temperature those doublets are equally populated; as the temperature decreases, the Kramers doublets of higher energy are successively depopulated, and the magnetic behavior significantly deviates from the Curie law predicted by the free-ion approximation.

The $\chi_M T$ values are 52.41 and 14.45 cm^3 K mol^{-1} for **2**·Gd and **2**·Nd at room temperature, respectively, close to the expected values of 52.52 and 15.07 cm^3 K mol^{-1} for noninteracting metal ions. The $\chi_M T$ value of **2**·Gd changes gradually from 52.41 cm^3 K mol^{-1} at 300 K to 49.00 cm^3 K mol^{-1} at 14 K, whereupon there is a more significant decrease to 33.56 cm^3 K mol^{-1} at 2.0 K. The data in the full measured temperature range 2−300 K are well fitted to the Curie−Weiss law with $C = 52.91$ and $\Theta = -1.13$ K, indicating very weak antiferromagnetic interactions. Differently, the $\chi_M T$ value of **2**·Nd decreases continuously on lowering the temperature, reaching a minimum value of 4.68 cm^3 K mol^{-1} at 2 K; the data in the range 60−300 K can be fitted to the Curie−Weiss law with $C = 16.86$ and $\Theta = -69.34$ K. Such overall antiferromagnetic behavior may be mainly attributed to antiferromagnetic interactions between Cu^{II}−Cu^{II} ion pairs, as well as the crystal-field effects around the Nd^{III} ion.[22b,25] In **2**·Gd, there are Cu−Cu and Cu−Gd interactions in $Cu_{12}Gd_6$ clusters. Furthermore, such $Cu_{12}Gd_6$ clusters are interconnected by dinuclear $Cu_2(OH)_2$ units. These interactions are too complicated for a detailed analysis; however, they cooperatively induce an observed antiferromagnetic behavior.

Discussion

Crystallizations of **1** and **2** at different conditions demonstrate that acidity of the reaction system is critically important in the formation of the final structure; a subtle change in acidity of the reaction solution can cause a drastic change in the structure of the product. In the current case, dinuclear **1**·Gd and **1**·Nd can be formed at a low pH value of ca. 3.5, whereas, at higher pH value (pH ≥ 6.5), hydroxide anions may participate in coordination to form the octadecanuclear $Cu_{12}Ln_6$ cores. Such phenomenon is parallel to our previous observations.[13−16] On the other hand, the pH is

(22) (a) Benelli, C.; Gatteschi, D. *Chem. Rev.* **2002**, *102*, 2369−2388. (b) Costes, J.-P.; Dahan, F.; Dupuls, A.; Laurent, J.-P. *Chem.—Eur. J.* **1998**, *4*, 1616−1620.
(23) Andruh, M.; Bakalbassis, E.; Kahn, O.; Trombe, J. C.; Pierre Porchers, P. *Inorg. Chem.* **1993**, *32*, 1616−1622.
(24) Paulovic, J.; Cimpoesu, F.; Ferbinteanu, M.; Hirao, K. *J. Am. Chem. Soc.* **2004**, *126*, 3321−3331.
(25) Kahn, M. L.; Mathoniere, C.; Kahn, O. *Inorg. Chem.* **1999**, *38*, 3692−3697.

slightly high in the syntheses of both **1** and **2** compared to those reported previously, which may be attributed to the difference between the carboxylate ligands. It is also worthy of note that upon changing of the ratio of the starting reagents, different heterometallic complexes may also be obtained, though further investigation is required.

In this work, Htza ligand was chosen as the carboxylate source for the formation of octadecanuclear $Cu_{12}Ln_6$ cores as well as for the further ligation using the tetrazole group to another metal center, leading to a polymeric structure based on the $Cu_{12}Ln_6$ cores. This ideal is realized with the formation of the dinuclear Cu^{II}_2 subunits between the Cu_{12}-Ln_6 cores, furnishing the 2D networks of **2** with the high-nuclearity nodes. Although the approach of assembling large polynuclear metal clusters into novel framework materials is still underdeveloped, a series of very recent examples of high-nuclearity 3d−4f heterometallic clusters as nodes for the construction of supramolecular networks are uncovered.[10] In these reports, different molecular designs and synthetic approaches were employed, leading to the interesting, high-nuclearity $[Ln_6Cu_{24}]$ octahedral-like clusters acting as the nodes and mononuclear $[Cu(AA)_2]$ (AA = amino acids) as the linkers, being different from the $Cu_{12}Ln_6$ cores and dinuclear Cu^{II}_2 subunits in **2**, respectively.

The magnetic behaviors of **1**·Gd and **2**·Gd are weakly overall antiferromagnetic, being similar to those reported for the Cu−Gd complexes of betaines.[14,16] In contrast, ferromagnetic interactions were found for Cu−Gd complexes of oxamates,[25] whereas the magnetic interaction in dinuclear Cu−Gd complexes made with compartmental Schiff base ligands is ferromagnetic in the large majority of published examples[8d,26] while an antiferromagnetic interaction is observed only in a few complexes.[27] Although we cannot explain fairly such a difference, one reasonable conclusion is that the weak magnetic interaction between Cu^{II} and Ln^{III} should be presented in a hydroxy-/carboxylate-bridged Cu^{II}−Ln^{III} system.

Conclusion

A new synthetic route was devised for constructing heterometallic high-nuclearity clusters into beautiful 2-D coordination architectures consisting of both octadecanuclear 3d−4f cores and dinuclear Cu^{II} cores that are interlinked by tza ligands. Our magnetic study suggests that there exist weak exchange interactions between the Cu^{II} and Ln^{III} ions with carboxylate and hydroxy bridges. On the other hand, the formation of the 2-D networks implies that, upon a suitable assembly approach, 3-D frameworks with large pores may be constructed with the high-nuclearity 3d−4f clusters, which may be of potential applications in absorption and catalysis. We are working toward related 3-D networks based on the nanosized clusters.

Acknowledgment. This work was supported by the National Natural Science Foundation of China (Grant No. 20131020), Ministry of Education of China (Grant No. 01134), and Scientific and Technological Bureau of Guangdong Province (Grant No. 04205405).

Supporting Information Available: An X-ray crystallographic file in CIF format. This material is available free of charge via the Internet at http://pubs.acs.org.

IC048754S

(26) Costes, J.-P.; Dahan, F.; Dupuls, A.; Laurent, J.-P. *Inorg. Chem*. **1997**, *36*, 3429−3433.
(27) Costes, J.-P.; Dahan, F.; Dupuls, A.; Laurent, J.-P. *Inorg. Chem*. **2000**, *39*, 169−173.